UCRL- 101932
PREPRINT

UCRL---101932

DE90 009183

RAILGUN PERFORMANCE WITH A TWO-STAGE LIGHT-GAS GUN INJECTOR

R. S. HAWKE
et. al.

5th Symposium on
Electromagnetic Launch Technology
Destin, FL

April 2-5, 1990

Lawrence Livermore National Laboratory

RAILGUN PERFORMANCE WITH A TWO-STAGE LIGHT-GAS GUN INJECTOR*+

R. S. Hawke and A. R. Susoeff
Lawrence Livermore National Laboratory
Livermore, CA

J. R. Asay, C. A. Hall, C. H. Konrad, and G. W. Wellman
Sandia National Laboratories, Albuquerque, NM

R. J. Hickman, W. A. Heath and J. R. Martinez
Ktech Corporation, Albuquerque, NM

J. L. Sauve' and A. R. Vasey
EG&G, Albuquerque, NM

M. Shahinpoor
University of New Mexico, Albuquerque, NM

ABSTRACT

This paper summarizes the results obtained with the HELEOS railgun which uses a two-stage light-gas gun (2SLGG) as an πinjector.[1] The high velocity 2SLGG injector preaccelerates projectiles up to ~8 km/s. The high injector velocity reduces the exposure duration of the railgun barrel to the passing high temperature plasma armature, thereby reducing the ablation and subsequent armature growth. The 2SLGG also provides a column of cool, high pressure hydrogen gas to insulate the rails behind the projectile, thereby eliminating restrike. A means to form an armature behind the injected projectile has been developed. In preliminary tests, the third stage railgun has successfully increased the projectile velocity by 1.35 km/s. Extensive diagnostics have been used to determine the behavior of the armature and track the launcher's performance. In some cases, velocity increases in the railgun section have been achieved, which are in close agreement with theoretical predictions, whereas in other experiments deviations from theoretical have been observed. The reasons for and implications of these results will be addressed. Recent tests are reported.

INTRODUCTION

STARFIRE is a joint Sandia National Laboratories, Albuquerque/Lawrence Livermore National Laboratory (SNLA/LLNL) program based at SNLA that has as its goal the development of a hypervelocity launcher for use as a high-pressure research tool [1, 2]. The launcher combines a two-stage light-gas gun (2SLGG) with a railgun. The 2SLGG is used as a projectile preaccelator/injector [1, 3], to the railgun. (The system is designated HELEOS-Hypervelocity Experimental Launcher for Equation Of State.)

The STARFIRE system uses the 2SLGG to minimize barrel ablation and armature contamination. Hydrogen is used as the propulsive injection gas, which provides injection velocities of 5 to 8 km/s and a nearly pure hydrogen environment immediately behind the projectile as it enters the railgun barrel. The hydrogen gas also serves to insulate the rails and thereby reduce the probability of forming secondary arcs.

*Work performed under the auspices of the U. S. Department of Energy by Lawrence Livermore National Laboratory under contract W-7405-ENG-48 and Sandia National Laboratories under contract DE-AC04-76DP00789.

+This Paper was prepared for presentation at the 5th Symposium on Electromagnetic Launch Technology to be held April 2-5, 1990 at Destin, FL.

REQUIREMENTS FOR SUCCESSFUL OPERATION

In order to successfully employ a 2SLGG as a hypervelocity injector followed by electromagnetic acceleration of a projectile, several challenges had to be met. The challenges included 1) refinement of the use of a 2SLGG in order to ensure the integrity of the projectiles; 2) development of the projectile sealing capability in order to minimize blowby; 3) elimination of pre-arcs in front of the projectile; and 4) development of a reliable means of forming a propulsive armature upon entrance into the railgun section. During the past two years, all of these challenges have been met and more than 15 significant tests with successful armature formation, most with significant electromagnetic velocity increases, have been performed.

DESCRIPTION OF THE PROJECTILE DESIGN

The most challenging task was the development of a means to reliably form a propulsive armature upon injection of the projectile into the railgun section. In the course of acceleration in the 2SLGG, a boundary layer between the projectile and barrel forms.[4, 5] This boundary layer is warm but not hot enough to be sufficiently conductive to commutate current. The boundary layer is relatively cool and non-conductive and tends to insulate any metal fuse or armature forming element on the backside of the projectile, thus inhibiting the most common means by which lower velocity injected projectile armatures are formed; metal foil fuses. We tested several methods of armature formation including spark discharge [6], barrel mounted metal fuse vapor injection [7] and the technique now in use, a seeded boundary layer commutation through a projectile mounted metalic armature. Fig. 1 is a lenghtwise sectional view of the projectile design [see figure caption for functional details]. This design has proven to be very reliable at commutating a rail-to-rail current flow after 2SLGG injection into the railgun section. A full band of conductive seeding material was used up through H62. The full band had a tendency to conduct current, vaporize and form an undesirable confined armature. From Test H63 onward only partial rings were used with good success.

MODES OF ARMATURE FUNCTION OBSERVED

The projectile shown in Fig. 1 has been observed to function in four modes; 1) hybrid with current passing through two short plasma brushes between the metal link and rails; 2) "pure" plasma serving as the sole current path; 3) tandem where a hybrid is closely followed by a plasma and both provide propulsion; and 4) confined where current passes through the seeding band. The later is not a desired mode and has been eliminated.

Fig. 2 is a muzzle voltage record which illustrates commutation and all four of the armature modes. The magnitude and duration of the initial commutation pulse indicates the difficulty of commutating current through the boundary layer (better seeding results in lower commutation voltage and shorter duration). A commutation voltage of ~900V is shown in Fig. 2 while more recent tasks have typically commutated at about 200 V. The subsequent high muzzle voltage indicates operation in a confined plasma mode [8]. The voltage drop to about 150V indicates operation in the hybrid mode [9]. The ramp up to ~240V is attributed to the rising plasma brush voltages associated with the increasing gap between the solid link and rails resulting from the erosion of the metal link and/or the recision of the rails away from the metal link. The recession is the result of pre-existing erosion of the rails from prior tests. When the voltage reaches ~240V it is clamped by a plasma armature which forms behind the hybrid. Gradually the plasma voltage decreases to about 200V and dominates until projectile launch.

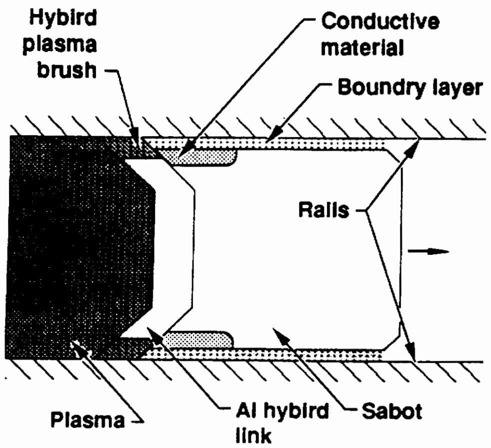

Fig. 1. Lengthwise section of projectile design illustrates the use of a thick Al disc attached to the back side of the plastic sabot to serve as the metal link of a hybrid armature. Conductive material is used to seed the boundary layer as it is eroded along with the sabot by the boundary layer. The seeding enables hybrid commutation at a few hundred volts. The Al armature first serves as the link for a hybrid armature. After a time, the ablated Al products feed the region behind the Al armature and as plasma conduction begins, evolves into a tandem (hybrid/plasma) armature. The plasma tends to stay in close proximity to the hybrid and contributes to the propulsion of the projectile.

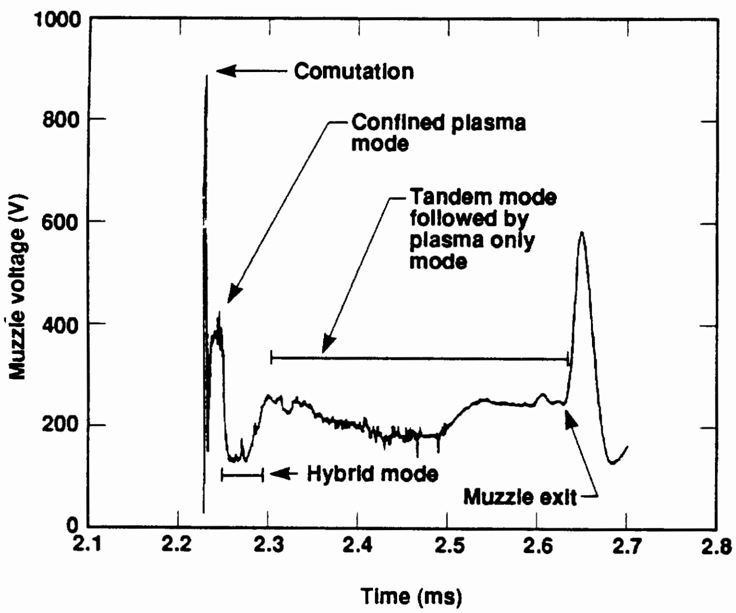

Fig. 2. Muzzle voltage vs. time record indicates mode of armature functioning. The first spike is associated with the rapid rise of the switched rail voltage until commutation between the rails occurs. In this case, a confined plasma is the first armature mode to occur. This mode results in a high armature voltage (~400v) and is followed by the formation of a hybrid mode at a lower voltage (~170v). The hybrid voltage ramps up as the plasma brush gaps become larger due to contact erosion and/or entrance into regions of the rails which are already eroded by previous tests. When the hybrid gaps are large enough to result in voltages exceeding a stable plasma voltage (~250v), the armature transitions into a tandem mode and possibly a pure plasma mode prior to launch.

ARMATURE PERFORMANCE RATIO

A useful (and important) method of comparing the results of tests with different injection velocities, armature types and armature modes is to calculate the ratio, ξ, of the measured electromagnetic velocity increase Δv to the maximum the theoretical velocity increase:

$$\xi = \frac{2m_p \Delta v}{L' \int I^2 dt}$$

where L' is the launcher inductance gradient, I is the current input to the railgun and m_p is the projectile mass. An ideal performance ratio (ξ = 100%) would indicate the full propulsion of all the current input to the railgun and a complete lack of parasitic losses such as; 1) viscous drag acting on the projectile and/or plasma(s); and 2) kinetic drag "m-dot" from erosion or ablation of the barrel by the projectile or plasmas and/or released surface layers by a bow shock traveling in front of the projectile. A loss of performance would also accompany a current diversion from the propulsive armature by a pre-arc infront of the projectile, restrike behind the armature, and/or a splitting of some or all of the current away from the rear of the propulsive plasma. In our tests, we have effectively eliminated pre-arc and restrike. Some of our tests have indicated that all the current remained in close proximity of the projectile while others have indicated a seperation or bifurcation of the armature into two or more regions.

TEST RESULTS

Fig. 3A and 3B are the direct arc and integrated rail magnetic probe records for HELEOS test H63. Fig. 3A is the composite of signals from eight arc B-dot probes oriented to sense only the magnetic field of armature current. Similarly, Fig. 3B is the overlaid composite records of eight integrated rail B-dot probes sensing only the rail current along with the total input current (dashed curve). The position of the eight pairs of probes are co-located and equally spaced. Fig. 3C is the normalized fraction of the rail current obtained by dividing each probe record shown in Fig. 3B by the instantaneous input current. Fig 3D is a summary plot of the position of; 1) the 1st and 2nd peaks and zero crossing of the arc B-dot records for the propulsive armature; and 2) the input current vs. time. In this case, a small bifurcation is seen starting to form on arc B-dot No. 3 but is absent at arc B-dot No. 4. Although not all of the available current was immediately behind the projectile (as seen in the integrated rail probe records 3B and 3C), the propulsive armature did remain with the projectile and contributed to projectile acceleration. Fig. 3C is a normalized version of 3B indicating the fraction of the input current sensed by each probe. The rapid rise of the 1st and 2nd probe current to 100% of the input current is consistent with operation in a hybrid mode. The finite rise time (7-9 μs) is limited by probe response [10, 11]. The 3rd probe indicates a rapid rising current up to about 65% of the input current followed by a more gradual increase to 100%. The gradual rise indicates a plasma tail behind the hybrid; hence, a tandem armature. The performance ratio of this test was about 30% and a velocity increase of 0.3 km/s was obtained.

Fig. 4A through 4D are again the same format as Fig.3A through 3D. The composite arc B-dot record (4A) indicates a relatively stable armature and the extinction of a small bifurcation that is seen in record No. 4 but absent in No. 5. On the other hand, the integrated rail B-dot record (4B) indicates a slight loss of propulsive armature current in records No. 2, 3 and 4 and significant loss in No. 5 and 6. Significant cumulative erosion of the rails from previous tests is located just past No. 2 and reaches a maximum at No. 4. The eroded rails result in larger hybrid gaps, higher armature (muzzle) voltage and may be the cause of an extended plasma current distribution behind the hybrid armature. The performance ratio of H65 was 65% and a velocity increase of 1.0 km/s was obtained.

In all cases, the full current input level is reached immediately behind the projectile or at a point close behind. No evidence of restrike is seen in any of the records. A lack of restrike might be the result of the hydrogen gas following the armature and/or the higher injection velocity.

Table 1

Test No.	40	41	45	48	49	52	54	55	56	61	62	63	64	65	66	78
Projectile Mass (grams)	2.39	2.11	2.81	2.44	2.63	2.40	2.37	1.67	2.06	2.14	2.18	2.28	2.36	2.54	2.17	2.28
Armature Thickness (mm)	0.66	0.66	1.09	0.66	1.09	1.09	1.09	0.10	1.52	1.09	1.09	1.09	1.09	1.52	1.52	1.52
Injection Velocity (km/s)	5.67	5.44	5.73	5.63	5.2	5.84	5.46	6.27	6.56	5.96	5.92	5.81	5.75	5.37	6.1	5.52
Launch Velocity (km/s)	6.07	5.64	6.28	5.63	5.47	6.04	5.98	6.12	7.21	6.43	6.75	6.71	6.51	6.37	6.66	6.89
Velocity Increase (km/s)	0.4	0.2	0.55	0	0.27	0.2	0.52	-0.15	0.65	0.47	0.83	0.90	0.76	1.0	0.56	1.35
Performance Ratio (Percent)	95	17	108	0	33	24	58	0	53	24	48	52	44	65	34	75
Peak Current (kA)	223	220, 230 *	280	230, 230 *	220, 230 *	320	315	290	340	430	427	410	423	408	386	435
Time to Peak Current From Main Bank (μs)	93	77, 141 *	89	105, 192 *	90, 190 *	94	84	122	109	112	102	90	98	110	100	96
Time to Bifurcation From Start Current (μs)	100	112		205	110	60		112			118					
From Start Current To Main Bank Fire (μs)	133	116, 181 *	135	155, 242 *	120, 220 *	94	144	180	175	150	140	97	133	145	105	110
Commutation Voltage (v)	750	934	940	1100	580	1130	970	1180	416	888	865	438	250	235	227	1190

*Indicates peak current and time of peak current for second pulse from time sequenced capacitor bank.

Table 1 is a numerical summary of 16 tests. In H78, a velocity increase of 1.35 km/s (5.52 km/s to 6.87 km/s) was measured for a 2.3g projectile along with an ξ of 75%. The performance ratio of H78 is about five times better than that obtained in the 1983 LLNL test F6 [12] where ξ had dropped to 15% while the projectile accelerated from 5.6 to 6.6 km/s. [Note: Although H40 and H45 indicate a large ξ, we believe some of the velocity again was the result of hydrodynamic boasts caused by; 1) rapid vaporization of the A1 armature during a fast rising current profile (H40); and 2) a rocket-like boost from a confined plasma (H45). Even though the confined mode provided a hydrodynamic velocity increase in H45, that was not generally the case as seen in H41, H48, H52, H55 and H61. These two effects were eliminated from all other tests. Formation of a confined plasma was eliminated by changing the conductive material used for seeding the boundary layer from a complete rail-to-rail band to an incomplete band, beginning with H63. In most tests, it was found that the velocity increase exceeded the theoretical value that would have been obtained if only the current flow in the hybrid were taken into consideration. Hence we conclude that at least some of the velocity increase is from the plasma behind the hybrid, especially in H63, H64, H65 and H66 where there was an absence of a confined armature (by design). Our hypothesis is that the plasma remains in contact with the projectiles and propulsive, at lease in part. This may be the result of plasma seeding by the "gradual" vaporization of the Al armature. Tests to fully differentiate these effects are in progress.

Fig. 5 is a summary of the measured velocity increase vs. the theoretically possible electromagnetic velocity increase including estimated error bars for each test. Fig. 6 is a compilation of the results from 15 tests.

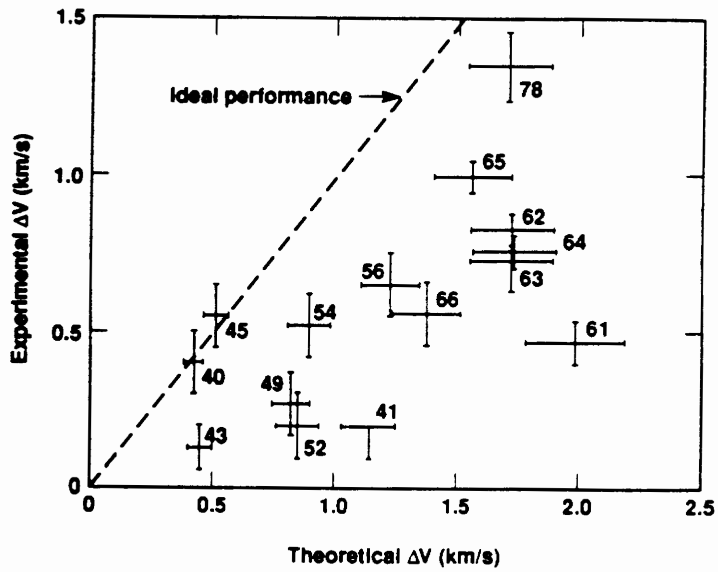

Fig. 5 Measured velocity increase vs. the theoretically possible electromagnetic velocity increase. The measured velocities are determined with fast pressure gauges and/or optical break beams at the input to the railgun and with flash X-Rays and/or MAVIS [13] velocity traps at the muzzle of the railgun. The measured input current is used to calculate the theoretical velocity gain.

CONCLUSIONS

The HELEOS system has successfully demonstrated the feasibility of using a 2SLGG as a hypervelocity injector for a railgun. This has opened the door to performing hypervelocity railgun tests without accumulated ablation products nor restrike in a velocity regime that heretofore has suffered enormous performance losses [11, 13, 14]. In the tests reported here, we have recorded a performance ratio of 75% (H78) which is a 5 fold improvement over tests done at LLNL in 1983. EOS system has also demonstrated the functioning of hybrid armatures at velocities greater than 6 km/s. This might be an indication that hybrids could be useful at high velocities even with low velocity injection.

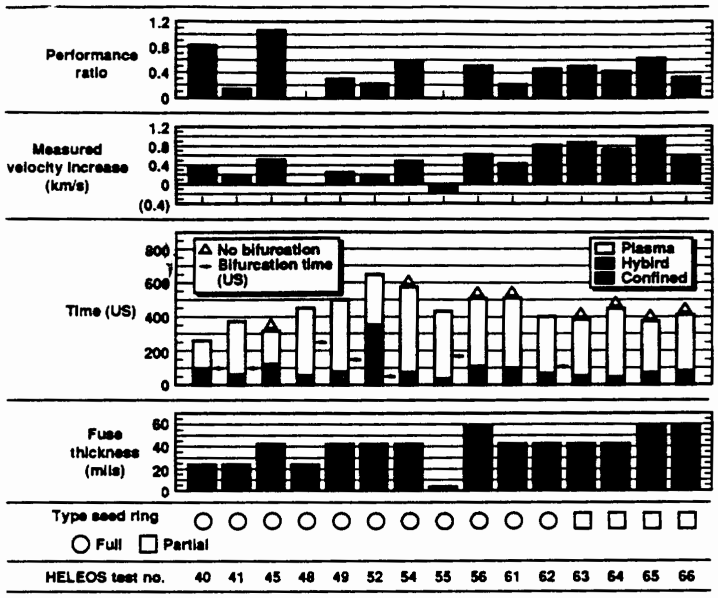

Fig. 6 Compilation of results from 15 tests. The bottom row indicates the test number; next row up the initial thickness of the Al armature. The third row is the approximate sequential time duration of each armature mode deduced from the muzzle voltage record. Bifurcation time, when it occurred and persisted, is indicated. The forth and fifth rows indicate the velocity gain and performance ratio respectively.

ACKNOWLEDGEMENTS

The support and encouragement of J. Chase, S. Cochran, D. Hayes and W. Herrmann have been instrumental in the execution of this project. The authors are pleased to acknowledge B. Clancy and G. W. Wellman for their valuable contributions to the project and C. Sanchez for preparing this manuscript.

REFERENCES

[1] R. S. Hawke, A. R. Susoeff, J. R. Asay, J. K. Balk, C. A. Hall, C. H. Konrad, M. J. McDonald, K. W. Schuler, G. W. Wellman, R. J. Hickman, M. Shanipoor and J. L. Sauve', "STARFIRE: Hypervelocity Railgun Development for High Pressure Research", IEEE Trans. on Mag., Mag-25(1) 223-227 (1989), pp. 643-648.

[2] R. S. Hawke, "Railgun Development for EOS Applications: A Status Report," *Shock Waves in Condensed Matter*, S. C. Schmidt and N. C. Holmes, Eds. (North Holland, Amsterdam, 1988), pp. 643-648.

[3] M. Shahinpoor, J. R. Asay,, C. H. Konrad and C. A. Hall, "Use of a Two-Stage Light-Gas Gun as an Injector for Hypervelocity Railguns", IEEE Trans. Mag., MAG-25(1), 514-518, (1989).

[4] A. C. Buckingham, "Electromagnetic Propulsion: Drag and Erosion Modeling, "AIAA J., 19(11), 1422-1428 (1981).

[5] S.- W. Kang and R. C. McCallen, "Plasma Behavior in the Boundary-Layer near a Railgun Surface" IEEE Trans. Mag., MAG - 25 (1), 217-297 (1989).

[6] R. S. Hawke, A. R. Susoeff, J. R. Asay, C. A. Hall, C. H. Konrad, R. J. Hickman, and J. L. Sauve', "Plasma Armature Formation in High-Pressure, High-Velocity Hydrogen", IEEE Trans. Mag., MAG-25(1), 219-227 (1989).

[7] R. S. Hawke, J. R. Asay, C. A. Hall, R. J. Hickman, C. H. Konrad, J. L. Sauve', and A. R. Susoeff, "Armature Formation in a Railgun Using a Two-Stage Light-Gas Gun Injector", IEEE Trans. Plasma Sci., 17(3), 378-385 (1989).

[8] F. D. Witherspoon, GT Devices, Alexandria, VA., private communication (1989).

[9] D. R. Keefer, University of Tenn, Tullahoma, TN., private communication (1989).

[10] J. V. Parker, "Magnetic-Probe Diagnostics for Railgun Plasma Armatures", *IEEE Trans. Plasma Sci,* 17(3), 487-500 (1989).

[11] L. M. Smith and D. R. Keefer, "Railgun Armature Plasma-Current Density from Deconvolved B-Dot Probe Signals", IEEE Trans. Plasma Sci., 17(3), 501-506 (1989).

[12] R. S. Hawke, W. J. Nellis, G. H. Newman, J. Rego and A. R. Susoeff, "Summary of EM Launcher Experiments Performed at LLNL", *IEEE Trans. Mag.,* MAG-22(6), 1510-1515 (1986).

[13] R. L. Moody and C. H. Konrad, "Magnetic Induction System for Two-Stage Gun Projectile Velocity Measurements", SAND 84-0638 Sandia National Laboratory, Albuquerque, NM 87185 (1984).

[14] G. A. Shvetsov, V. M. Titov, A. G. Anisimov, Yu. L. Bashkatov and I. A. Stadnichenko, "Railgun Accelerators of Macroparticules; Part II. Experimental Investigations," Megagauss Technology and Pulse Power Applications, C. M. Fowler, R. S. Caird, and D. J. Erickson, Eds. (Plenum Press, New York, 1987), pp. 795-801.

[15] M. M. Kondratenko, E. F. Lebedev, V. E. Ostashev, V. I. Safonov, A. V. Ul'anov, and V. E. Fortov, "Dynamic Features of Projectile Acceleration in an Arc-Driven Railgun", Megagauss Technology and Pulse Power Applications, C. M. Fowler, R. S. Caird, and D. J. Erickson, Eds. (Plenum Press, New York, 1987) pp. 811-817.

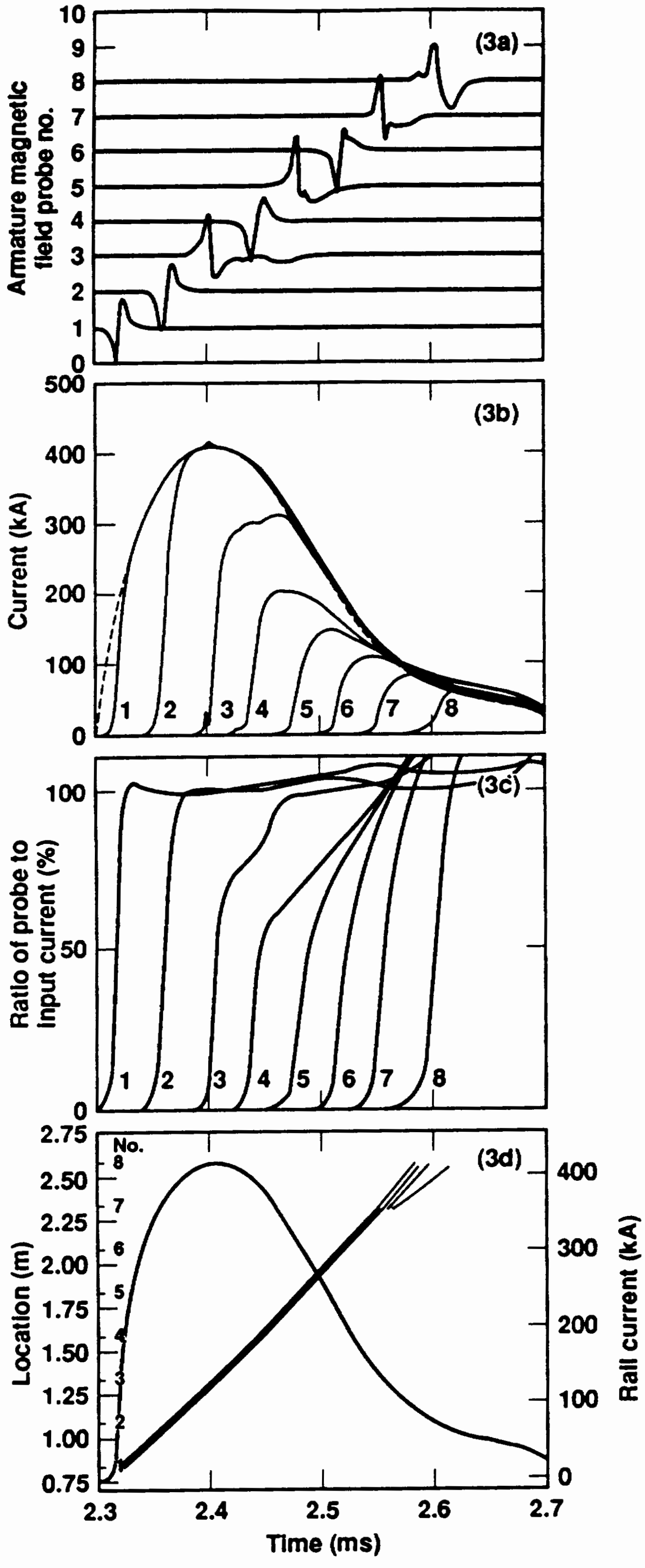

Fig. 3. Test results for H63. The performance ratio of this test was about 30% and a velocity increase of 0.3 km/s was obtained.

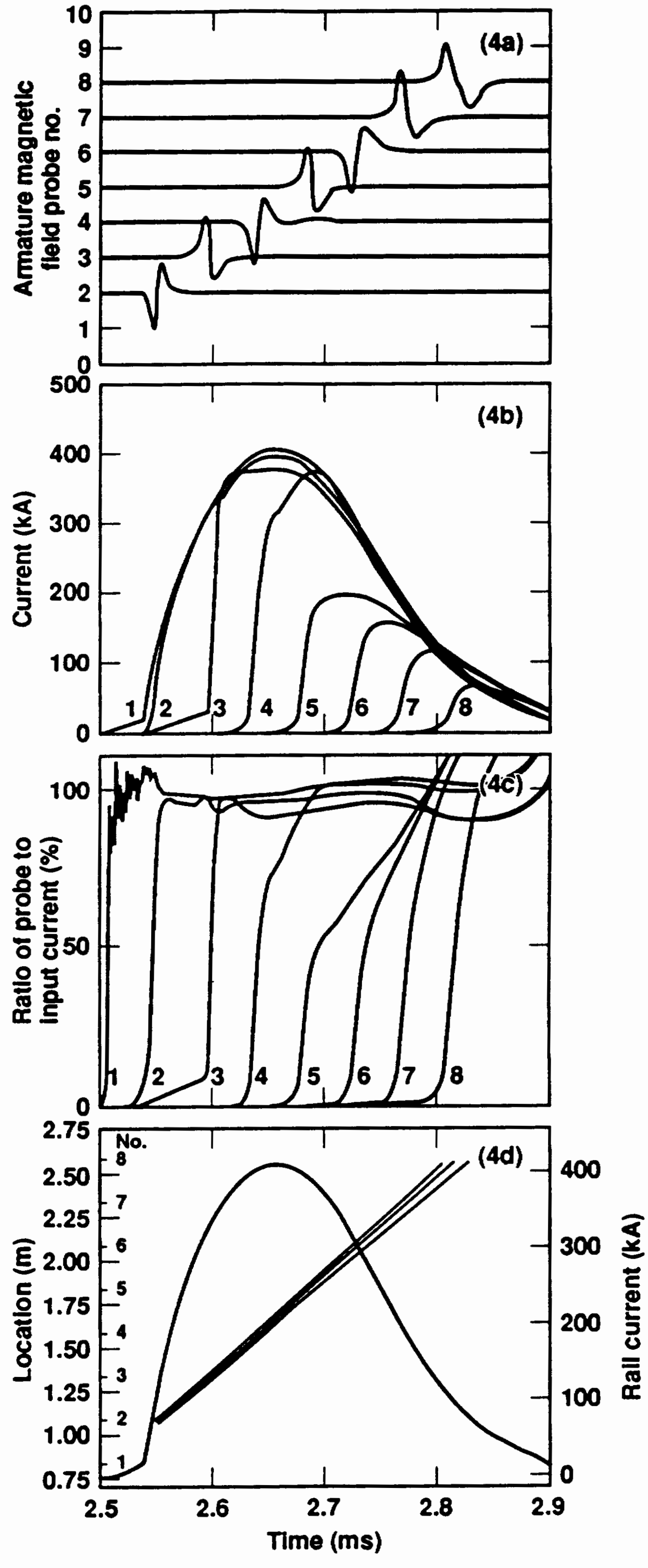

Fig. 4. Test results for H65. This test had a performance ratio of 65% and a velocity increase of 1.0 km/s.